Novel diamondoid-based maturity models using naturally occurring petroleum fluids

Robin van der Ploeg, Jos B. M. Pureveen, Sander H. J. M. van den Boorn, and Pim F. van Bergen

ABSTRACT

Diamondoids have been extensively used in petroleum geochemistry for thermal maturity assessment of hydrocarbon fluids and the source rocks from which they are derived. Both diamondoid concentrations and diamondoid indices have been proposed as maturity indicators, but no relationships have been shown to be universally applicable across multiple petroleum systems and source rock types. Here, we present a new quantitative maturity calibration for fluids from marine source rocks, based on diamondoids data from oils and gas condensates produced across a well-constrained maturity gradient of 0.5% to 1.5% vitrinite reflectance equivalent (VRE) in a combination of conventional and unconventional plays.

We systematically examine the relationships between diamondoid compositions and VRE as estimated from source rock measurements and basin models and observe distinct maturity ranges for generation and destruction of diamondoids of increasing carbon numbers. Notably, the absolute concentrations of ethyl-substituted adamantane isomers display the strongest and most consistent maturity relationships across all petroleum systems included in our data set.

Four new diamondoid maturity models are proposed, of which the most promising is based on the relative abundances of adamantane and its suspected precursor, perhydrotriquinacene. We call this parameter the adamantane index and find that it displays an excellent relationship to VRE in our data set (adjusted coefficient of determination of 0.87) that is superior to the performance of all previously established diamondoid indices.

Collectively, our work represents a major advance in understanding the evolution of diamondoid distributions in naturally occurring hydrocarbon fluids and enables better quantitative maturity estimation using an integrated diamondoid workflow for exploration and production geochemistry applications.

Copyright ©2023. The American Association of Petroleum Geologists. All rights reserved. Gold Open Access. This paper is published under the terms of the CC-BY license.

Manuscript received January 6, 2023; final acceptance February 7, 2023.
DOI:10.1306/06272323003

AUTHORS

Robin van der Ploeg ~ *Shell Global Solutions International B.V., Amsterdam, the Netherlands; R.vanderPloeg@shell.com*

Robin van der Ploeg is a geochemist at Shell and is currently based in Amsterdam, the Netherlands. He obtained both his M.Sc. degree in geology and Ph.D. in geochemistry at Utrecht University. He has broad research interests and has worked at the interface of multiple disciplines including petroleum geology, paleoclimatology, and earth system modeling. Since joining Shell in 2019, Robin has successfully developed new geochemical technologies and workflows to support the upstream business and has been involved in various geochemistry initiatives for the energy transition.

Jos B. M. Pureveen ~ *Shell Global Solutions International B.V., Amsterdam, the Netherlands; Jos.Pureveen@shell.com*

Jos B. M. Pureveen is a researcher in the geochemistry experimentation team at Shell. He has 25 years of experience in a variety of gas chromatographic and mass spectrometric techniques. Jos was closely involved in the analytical developments that enabled the diamondoid technology presented here.

Sander H. J. M. van den Boorn ~ *Shell Global Solutions International B.V., Amsterdam, the Netherlands; Sander.Van-Den-Boorn@shell.com*

Sander H. J. M. van den Boorn is team lead of the geochemistry experimentation team and subject matter expert for inorganic and analytical geochemistry at Shell. In his 14 years at Shell, he has worked in both research and business support functions and has focused on the development and deployment of novel geochemical tools. Sander leads a team responsible for the state-of-the-art geochemical laboratory at Energy Transition Campus Amsterdam, supporting technology development in the Upstream and energy transition domains.

PIM F. VAN BERGEN ~ *Shell Research Ltd., Aberdeen, United Kingdom; Pim.vanBergen@shell.com*

Pim F. van Bergen is the principal technical expert for geochemistry at Shell. He obtained his M.Sc. degree in biology from Utrecht University and a Ph.D. in organic geochemistry at Royal Holloway, University of London. He has worked for more than 30 years in the upstream business including for more than 20 years at Shell. Apart from geochemistry he has also worked in flow assurance and used geochemical tools to solve issues from exploration and development to decommissioning and downstream fluid production allocation.

ACKNOWLEDGMENTS

We acknowledge Rolande Dekker and Erik Tegelaar for foundational analytical method developments on diamondoids technology in Shell Global Solutions International B.V. and Johan Weijers and Mathew Fay for discussions on sample selection and interpretation at Shell. In addition, we thank AAPG associate editor Kenneth E. Peters, reviewer Craig D. Berrie, and an anonymous reviewer for supporting the publication of this paper.

DATASHARE 169

Figures S1 and S2, Tables S1 and S2, and Supplementary Data 1 are available in an electronic version on the AAPG website (www.aapg.org/datashare) as Datashare 169.

INTRODUCTION

Diamondoids are caged hydrocarbons that occur naturally in petroleum fluids and were first discovered in Czechoslovakian crude oil (Landa and Macháček, 1933). Because of their resistance to both thermal degradation and biodegradation, diamondoids are present in petroleum fluids of virtually all thermal maturity levels and under a wide range of geological conditions (Peters et al., 2005). Hence, diamondoids have been extensively used in petroleum systems analysis. Key areas of investigation include the thermal maturity assessment of hydrocarbon fluids or their source rocks (Chen et al., 1996; Zhang et al., 2005; Wei et al., 2006, 2007b; Mankiewicz et al., 2009; Fang et al., 2013; Jiang et al., 2021), estimation of the extent of fluid cracking (Dahl et al., 1999; Fang et al., 2012), distinguishing source rock facies (Schulz et al., 2001), establishing fluid–fluid and fluid–source rock correlations (Moldowan et al., 2015; Esegbue et al., 2020; Spaak et al., 2020; Botterell et al., 2021; Forkner et al., 2021), determining the degree of fluid biodegradation (Williams et al., 1986; Grice et al., 2000; Wei et al., 2007a; Cheng et al., 2018), and deconvolving fluid mixtures of low-mature and high-mature components (Atwah et al., 2021). Collectively, diamondoids record relevant geological information in their absolute concentrations, concentration indices, and carbon isotopic compositions ($\delta^{13}C$), but as with many other geochemical parameters, we know of no relationships that are universally applicable across multiple petroleum systems and source rock types.

Recent studies have focused on refining the compounding effects of thermal maturity and organic matter type on diamondoid distributions through laboratory-based pyrolysis experiments of kerogen (Jiang et al., 2018) and multivariate statistical analyses to develop predictive models for naturally occurring petroleum fluids (Jiang et al., 2021). Here, we further advance this effort by presenting a new diamondoid-based quantitative maturity calibration for naturally occurring petroleum fluids derived from marine source rocks. This has been uniquely developed using produced oils and gas condensates that are obtained across well-constrained maturity gradients in a combination of conventional and unconventional plays. As such, our calibration is expected to be more directly representative of the natural variability within and between petroleum systems and may thus be able to perform better in absolute thermal maturity prediction than models presented in previous studies based on kerogen heating experiments.

METHODS

Samples

A total of 91 hydrocarbon fluid samples were chosen for this study from a selection of petroleum systems across the world

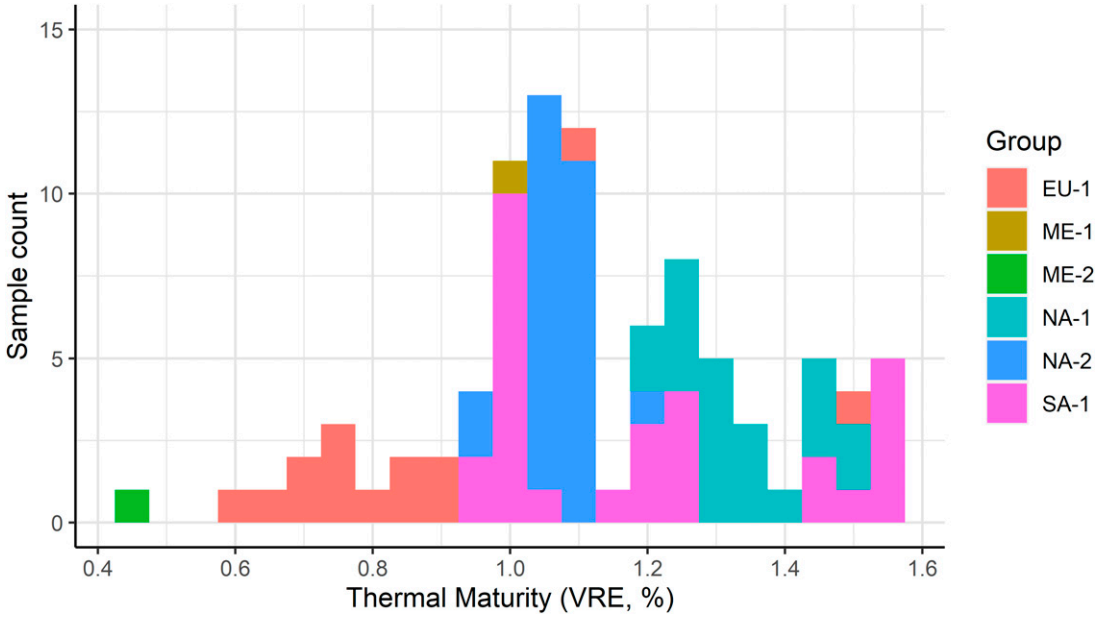

Figure 1. Fluid sample distribution against thermal maturity and split per region of origin (cf. Table 1). EU = Europe; ME = Middle East; NA = North America; SA = South America; VRE = vitrinite reflectance equivalent.

(Figure 1; Table 1). Good source rock type and thermal maturity control is key and therefore our sample set was predominantly focused on fluids from unconventional systems where paired rock and fluid data types were available and integrated in a basin-modeling framework. Specifically, the following criteria were used to evaluate whether fluid samples were suitable for inclusion in our study: (1) the corresponding source rock has been confidently identified; (2) the fluid represents a single charge; (3) reservoir alteration processes such as biodegradation have not been observed; and (4) a quantitative thermal maturity estimate is available, either in the form of source rock vitrinite reflectance (VR) measurements or as VR equivalent (VRE) inferred from a basin model or other geochemical fluid parameters, with uncertainty less than 0.1% VRE. The full sample set spans a thermal maturity range of 0.45% to 1.55% VRE and thus encompasses the full maturity spectrum of liquid petroleum fluids, from early oil generation to gas condensate formation.

Analyses

All petroleum fluid samples were prepared and analyzed at Energy Transition Campus Amsterdam, the Netherlands. In summary, an aliquot of ~50 ml crude oil or condensate was weighed in a glass vial, after which a known amount of internal standard solution (perdeuteroadamantane dissolved in cyclohexane) was added for quantification. The perdeuteroadamantane standard was acquired from CDN Isotopes (product no. D1165). Subsequently, samples were dissolved in cyclohexane, and the saturated hydrocarbon fraction

Table 1. Hydrocarbon Fluids Included in This Study

Region	Group	Petroleum System Type	Sample Count	Source Rock Age	Kerogen Type	VRE Range, %
South America	SA-1	Unconventional	29	Jurassic	Type II	0.9–1.6
North America	NA-1	Unconventional	20	Devonian	Type II	1.2–1.5
North America	NA-2	Conventional	26	Jurassic	Type II	0.9–1.2
Middle East	ME-1	Unconventional	1	Silurian	Type II	1.0
Middle East	ME-2	Unconventional	1	Cenozoic	Type IIS	0.4–0.5
Europe	EU-1	Conventional	14	Jurassic	Type II	0.6–1.5

Abbreviation: VRE = vitrinite reflectance equivalent.

containing diamondoids was isolated through solid phase extraction using activated silver nitrate silica gel as sorbent (silver nitrate acquired from Acros [product no. 19768] and silica gel from Agilent [40 µm particle size, product no. 12213001]) and cyclohexane as eluent. These saturated hydrocarbon fractions were further purified into branched/cyclic fractions by adding molecular sieves (Merck, 1.05705 Å) to selectively remove n-alkanes (≥12 hr reaction time).

Diamondoids were measured on the branched/cyclic fractions using two-dimensional gas chromatography (Agilent 7890A GC gas chromatograph [GC]) coupled to a mass selective detector (Agilent 5975C MSD mass selective detector [MSD]). The two-dimensional gas chromatography (GC×GC)-MSD instrument was operated in a reverse column setup (first column: polar, 20 m Agilent DB-17ms column with 0.25-mm internal diameter [ID] and 0.25 µm film thickness [Df]; second column: apolar, 3.7 m Agilent DB-1ms column with 0.1-mm ID and 0.1 µm Df), with the mass selective detector set to selective ion monitoring. Modulation was performed using a ZOEXII thermal modulator, with modulation time set to 10-s intervals. Electron voltage was maintained at 70 eV, the source temperature of the mass selective detector at 230°C, the interface temperature at 280°C, and the quadrupole temperature at 150°C. Sample injection into the GC×GC system was performed using 1 µl aliquots (splitless) at 250°C and the gas chromatograph oven temperature was set to increase from 60°C to 300°C using a linear oven temperature ramp of 2°C/min. Helium was used as the carrier gas with a flow rate of 0.7 ml/min. Total analysis time per sample was 131 min.

Analysis with GC×GC-MSD allowed for excellent separation and identification of individual diamondoid compounds (Figures S1, S2; Tables S1, S2; supplementary material available as AAPG Datashare 169 at www.aapg.org/datashare). Quantification of diamondoids was performed on a peak area basis, by comparing the peak areas for individual compounds and compound groups to the peak area of the internal standard (perdeuteroadamantane). Perhydrotriquinacene (PTQ) was identified based on a combination of both its elution order relative to adamantane and its mass spectrum (Figure S2, supplementary material available as AAPG Datashare 169 at www.aapg.org/datashare), which has distinctive mass-to-charge ratio (*m/z*) 80 and 108 fragments related to the consecutive loss of two ethene fragments from the PTQ molecular ion (*m/z* 136).

Long-term monitoring of in-house standard oils was employed to assure data quality and assess the external reproducibility of all diamondoid parameters for the samples investigated (Figure 2). Based on a total of 76 replicate analyses of three different standard oils over the study period, the analytical uncertainty was found to be typically ≤10% of the absolute

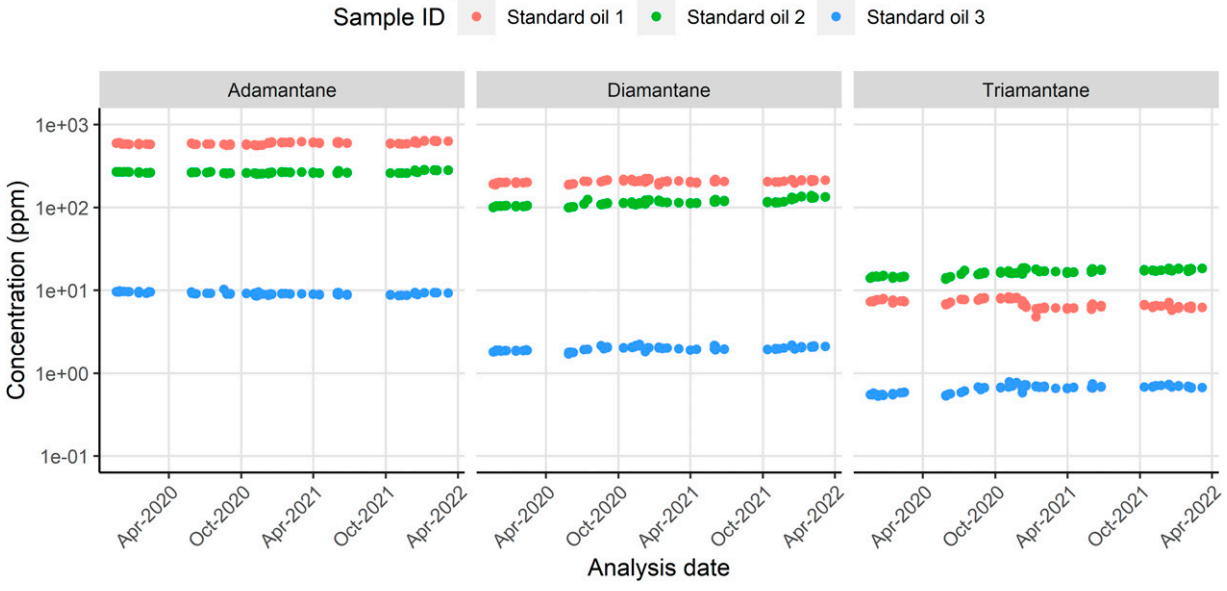

Figure 2. Analytical reproducibility for quantification of adamantane, diamantane, and triamantane over the course of the study period, tracked using three different standard oils. Apr = April; ID = identifier; Oct = October.

concentration of a given diamondoid compound (1 standard deviation). Statistical evaluation of the data set was performed in R, a language and environment for statistical computing (R Core Team, 2022) and figures were produced using the ggplot2 package (Wickham, 2009). All data reported in this study are included in Supplementary Data 1 (supplementary material available as AAPG Datashare 169 at www.aapg.org/datashare).

RESULTS

Diamondoid Distributions

Diamondoids were successfully detected and quantified in the adamantane to tetramantane range across all samples (Figure 3). Generally, we find that total adamantane and diamantane concentrations show a progressive increase in abundance over the full maturity range investigated. By contrast, total triamantane and tetramantane concentrations show an initial increase up to a maximum abundance at a VRE maturity of ~1.0% (corresponding to peak oil window), after which concentrations start to decline. Absolute diamondoid concentrations are thus strongly correlated with thermal maturity in our data set, and these relationships appear to be largely shared between the fluids from the different petroleum systems. This suggests that the diamondoid distributions in these fluids indeed share a common thermal maturity control, with limited effects from inter- and intrabasinal source-rock type variations. However, we note that a single fluid from the Middle East-2 group appears to be a relative outlier, potentially because it is derived from a type IIS source rock that is virtually immature (VR ~0.45%).

Similarly, the diamondoid parameters developed in previous studies (Chen et al., 1996; Schulz et al., 2001; Zhang et al., 2005; Mankiewicz et al., 2009) appear to increase with thermal maturity in our data set, but differences are observed between the adamantane-based and diamantane-based indices (Figures 4, 5; see Tables S1, S2 for parameter definitions, supplementary material available as AAPG Datashare 169 at www.aapg.org/datashare). Most adamantane-based indices increase linearly over the investigated maturity range and behave relatively consistently across the different petroleum systems, except for the fluids from the North America-2 group (Figure 4). Strikingly, the diamantane-based indices show little variability, which prevents establishing any real relationships over the maturity range covered by our data set. The integrated bridgehead-to-secondary (BTS) carbon isomerization parameters BTS-1 and BTS-2 (Mankiewicz et al., 2009) also show similar outcomes (Figure 5), including a diminished response in the diamantane-based BTS-2 ratio compared to the adamantane-based BTS-1 ratio.

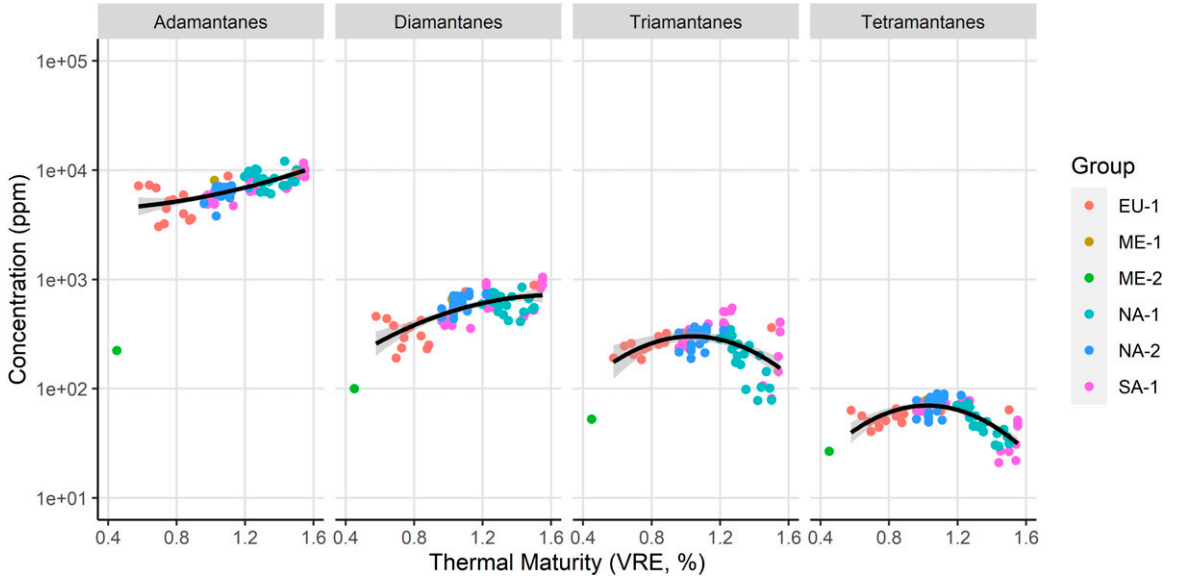

Figure 3. Overview of absolute diamondoid concentrations versus thermal maturity for all fluids. Solid black lines represent second-degree polynomial fits to all data to highlight the main trends (excluding the outlier sample from the Middle East [ME]-2 group in green), with 95% confidence intervals of the fits in gray shading. EU = Europe; NA = North America; SA = South America; VRE = vitrinite reflectance equivalent.

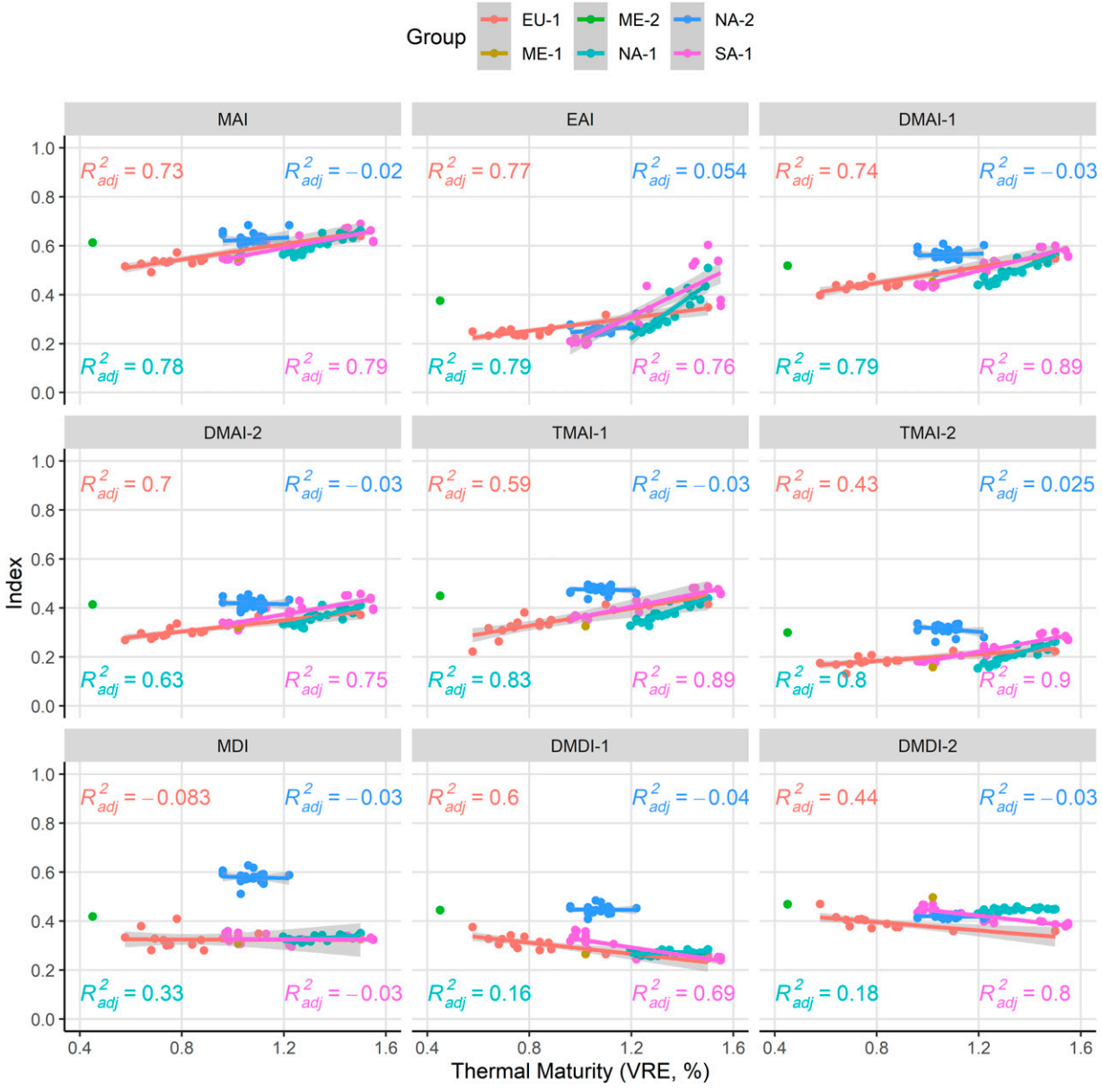

Figure 4. Overview of methyladamantane index (MAI), ethyladamantane index (EAI), dimethyladamantane index 1 (DMAI-1), dimethyladamantane index 2 (DMAI-2), trimethyladamantane index 1 (TMAI-1), trimethyladamantane index 2 (TMAI-2), methyldiamantane index (MDI), dimethyldiamantane index 1 (DMDI-1), and dimethyldiamantane index 2 (DMDI-2) parameter results versus thermal maturity for all fluids. The *y* axes are identical in all panels. Solid lines represent linear fits to the data for each regional group, with 95% confidence intervals of the fits in gray shading. EU = Europe; ME = Middle East; NA = North America; R^2_{adj} = adjusted coefficient of determination; SA = South America; VRE = vitrinite reflectance equivalent.

We even find that the methyladamantane/adamantane (MA/A) and methyldiamantane/diamantane (MD/D) parameters, which were previously found to increase with fluid biodegradation rank (Grice et al., 2000), are related to thermal maturity (Figure 6). However, a potential compounding effect of both maturity and biodegradation on these parameters cannot be precluded since we specifically selected our calibration sample set to exclude biodegraded fluids.

Novel Maturity Parameters

The relationships we observe in our data set lead us to propose a set of new diamondoid maturity parameters. Here, we explicitly exclude the one fluid

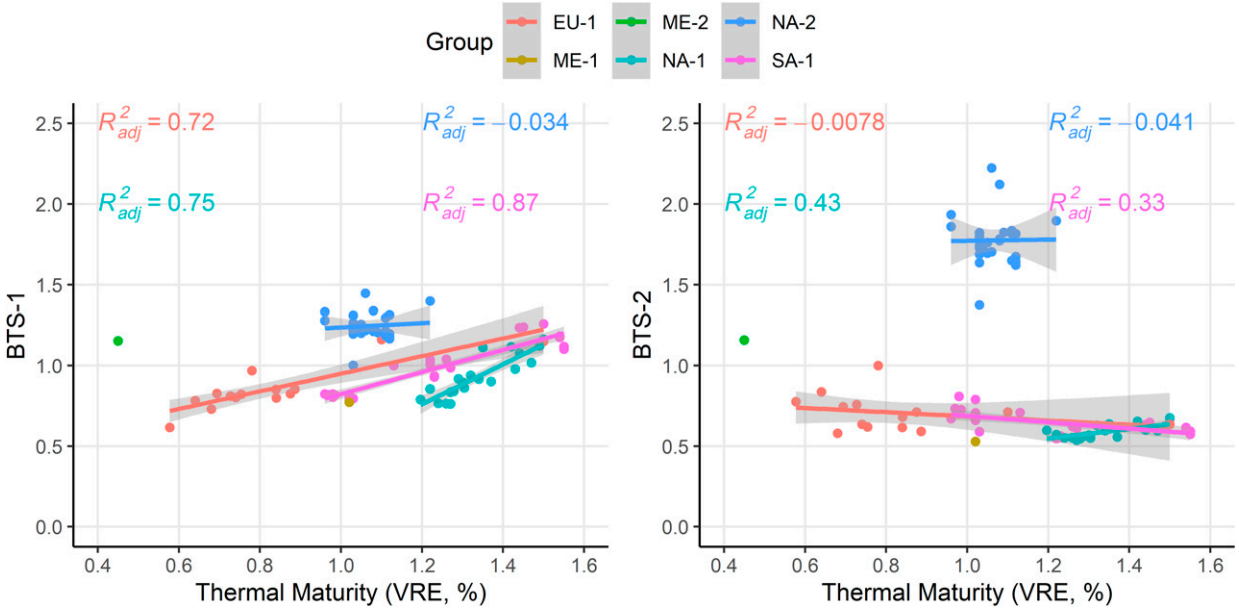

Figure 5. Bridgehead-to-secondary (BTS) carbon isomerization parameters BTS-1 and BTS-2 versus thermal maturity for all fluids. The *y* axes are identical in all panels. Solid lines represent linear fits to the data for each regional group, with 95% confidence intervals of the fits in gray shading. EU = Europe; ME = Middle East; NA = North America; R^2_{adj} = adjusted coefficient of determination; SA = South America; VRE = vitrinite reflectance equivalent.

from group ME-2 in the calibration of these new parameters because of its generally anomalous diamondoid compositions compared to the rest of the data set.

Three new indices are proposed based on the relative stability differences between ethyladamantane isomers and methyladamantane isomers of C2-, C3- and C4-adamantanes. This relies on the notion that all adamantanes eventually rearrange to their most stable methyladamantane isomer via the ethyladamantane isomer with the same number of carbon

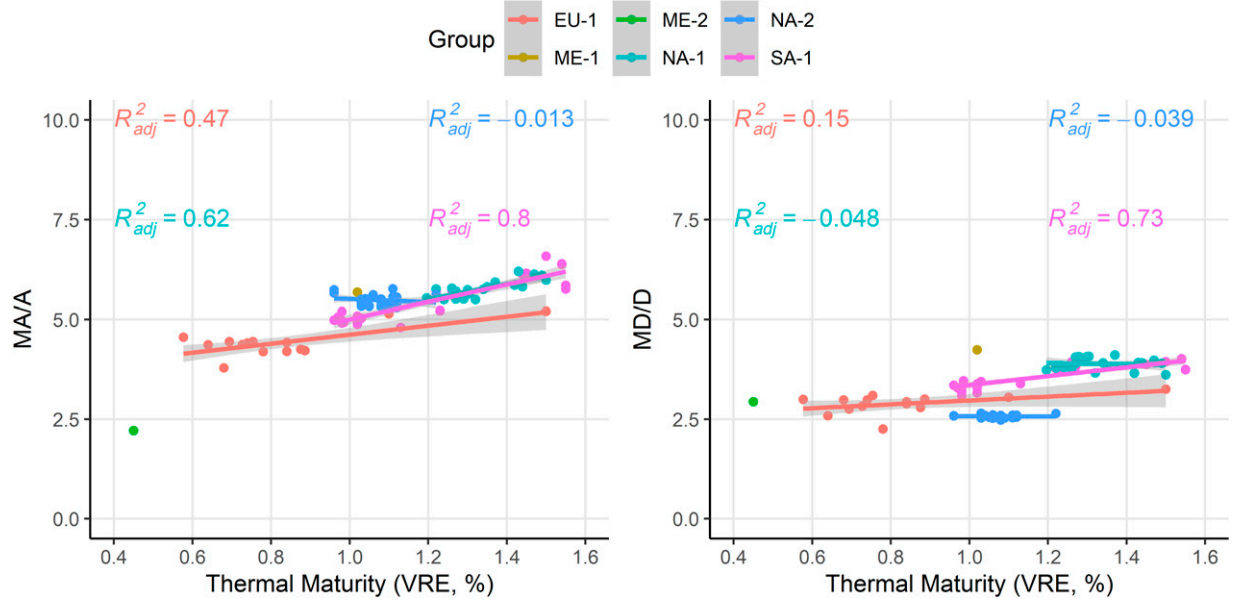

Figure 6. Methyladamantane/adamantane (MA/A) and methyldiamantane/diamantane (MD/D) parameter results versus thermal maturity for all fluids. Solid lines represent linear fits to the data for each regional group, with 95% confidence intervals of the fits in gray shading. EU = Europe; ME = Middle East; NA = North America; R^2_{adj} = adjusted coefficient of determination; SA = South America; VRE = vitrinite reflectance equivalent.

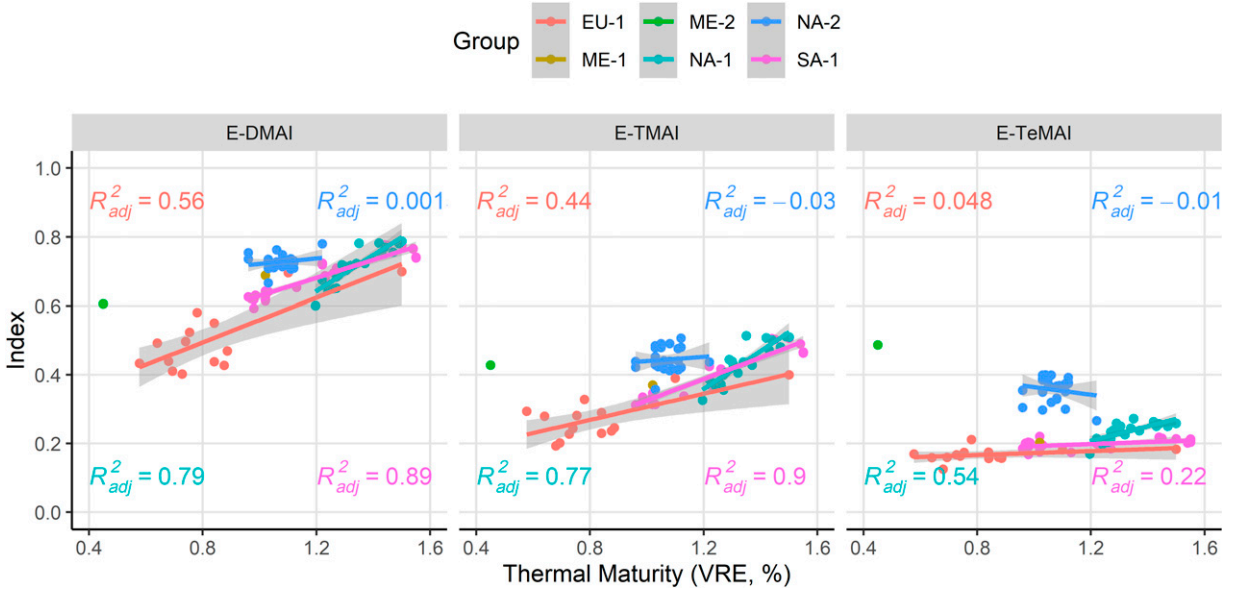

Figure 7. The newly proposed ethyl-dimethyladamantane index (E-DMAI), ethyl-trimethyladamantane index (E-TMAI), and ethyl-tetramethyladamantane index (E-TeMAI) parameters versus thermal maturity for all fluids. Solid lines represent linear fits to the data for each regional group, with 95% confidence intervals of the fits in gray shading. EU = Europe; ME = Middle East; NA = North America; R^2_{adj} = adjusted coefficient of determination; SA = South America; VRE = vitrinite reflectance equivalent.

atoms (Schneider et al., 1964). For instance, the reactions that lead to the formation of 1,3-dimethyladamantane (1,3-DMA), 1,3,5-trimethyladamantane (1,3,5-TMA), and 1,3,5,7-tetramethyladamantane (1,3,5,7-TetraMA) have been suggested to occur via 1-ethyladamantane (1-EA), 1-ethyl-3-methyladamantane (1-E-3-MA), and 1-ethyl-3,5-dimethyladamantane (1-E-3,5-DMA), respectively (Schneider et al., 1964). Here, we employ this concept to design the following three indices, which we call ethyl-dimethyladamantane index (E-DMAI), ethyl-trimethyladamantane index (E-TMAI), and ethyl-tetramethyladamantane index (E-TeMAI), respectively:

$$\text{E-DMAI} = 1,3\text{-DMA}/(1,3\text{-DMA} + 1\text{-EA}) \quad (1)$$

$$\text{E-TMAI} = 1,3,5\text{-TMA}/(1,3,5\text{-TMA} + 1\text{-E-3-MA}) \quad (2)$$

$$\text{E-TeMAI} = 1,3,5,7\text{-TetraMA}/(1,3,5,7\text{-TetraMA} + 1\text{-E-3,5-DMA}) \quad (3)$$

The E-DMAI and E-TMAI parameters both have relatively strong correlations with maturity, whereas E-TeMAI performs less well given its reduced parameter space (Figure 7). However, this new set of ethyladamantane maturity parameters appears to not be fully representative across all petroleum systems in our data set, similar to the established diamondoid maturity parameters (Figures 4–6). Furthermore, a progressive decrease in the absolute concentrations of the respective ethyladamantane isomers with fluid maturity is not observed, as might be suspected from the aforementioned theory (Schneider et al., 1964). Remarkably, we find that 1-EA, 1-E-3-MA, and 1-E-3,5-DMA as well as 1-E-3,5,7-TMA concentrations all increase exponentially with maturity and even display globally consistent maturity relationships across our full data set (Figure 8). This suggests that individual ethyladamantane isomer abundances may potentially be used directly for quantitative maturity prediction.

In addition, we propose a new maturity parameter based on the relative abundances of adamantane and one of its suspected precursor molecules, PTQ. The PTQ has a structure consisting of three fused cyclopentane rings in the shape of a shallow bowl and has been described previously as a precursor in a series of transformation reactions of tricyclodecane isomers to adamantane (Whitlock and Siefken, 1968; Paquette et al., 1969; Engler et al., 1973; Clark et al., 1979). To the best of our knowledge, PTQ has not been reported or quantified in any subsequent

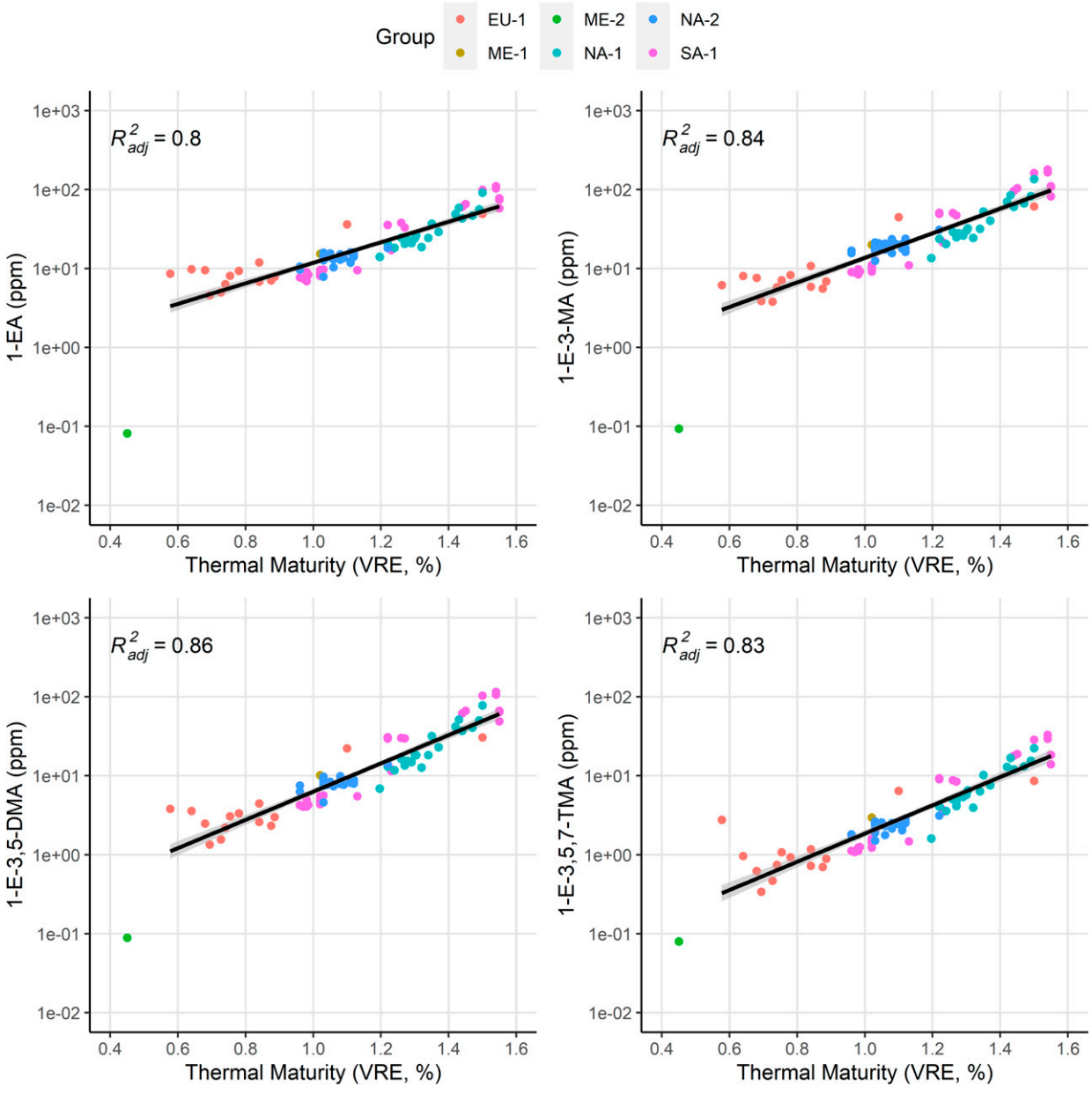

Figure 8. Concentrations of ethyladamantane isomers 1-ethyladamantane (1-EA), 1-ethyl-3-methyladamantane (1-E-3-MA), 1-ethyl-3,5-dimethyladamantane (1-E-3,5-DMA), and 1-ethyl-3,5,7-trimethyladamantane (1-E-3,5,7-TMA) shown versus thermal maturity for all fluids. Solid black lines represent linear fits to all data (excluding the outlier sample from the Middle East [ME]-2 group in green), with 95% confidence intervals of the fits in gray shading. EU = Europe; NA = North America; R^2_{adj} = adjusted coefficient of determination; SA = South America; VRE = vitrinite reflectance equivalent.

petroleum geochemistry studies, but we observe it in all studied samples regardless of fluid maturity. The concentration of adamantane increases exponentially with maturity in our data set, whereas PTQ remains virtually invariant (Figure 9), potentially because of its inferred endothermic reaction pathway (Engler et al., 1973). These differences between adamantane and PTQ result in a particularly strong maturity relationship in their relative proportions. We therefore define a new parameter that we call the adamantane index (AI), expressed as

$$\mathrm{AI} = \mathrm{A}/(\mathrm{A} + \mathrm{PTQ}) \quad (4)$$

where A is adamantane.

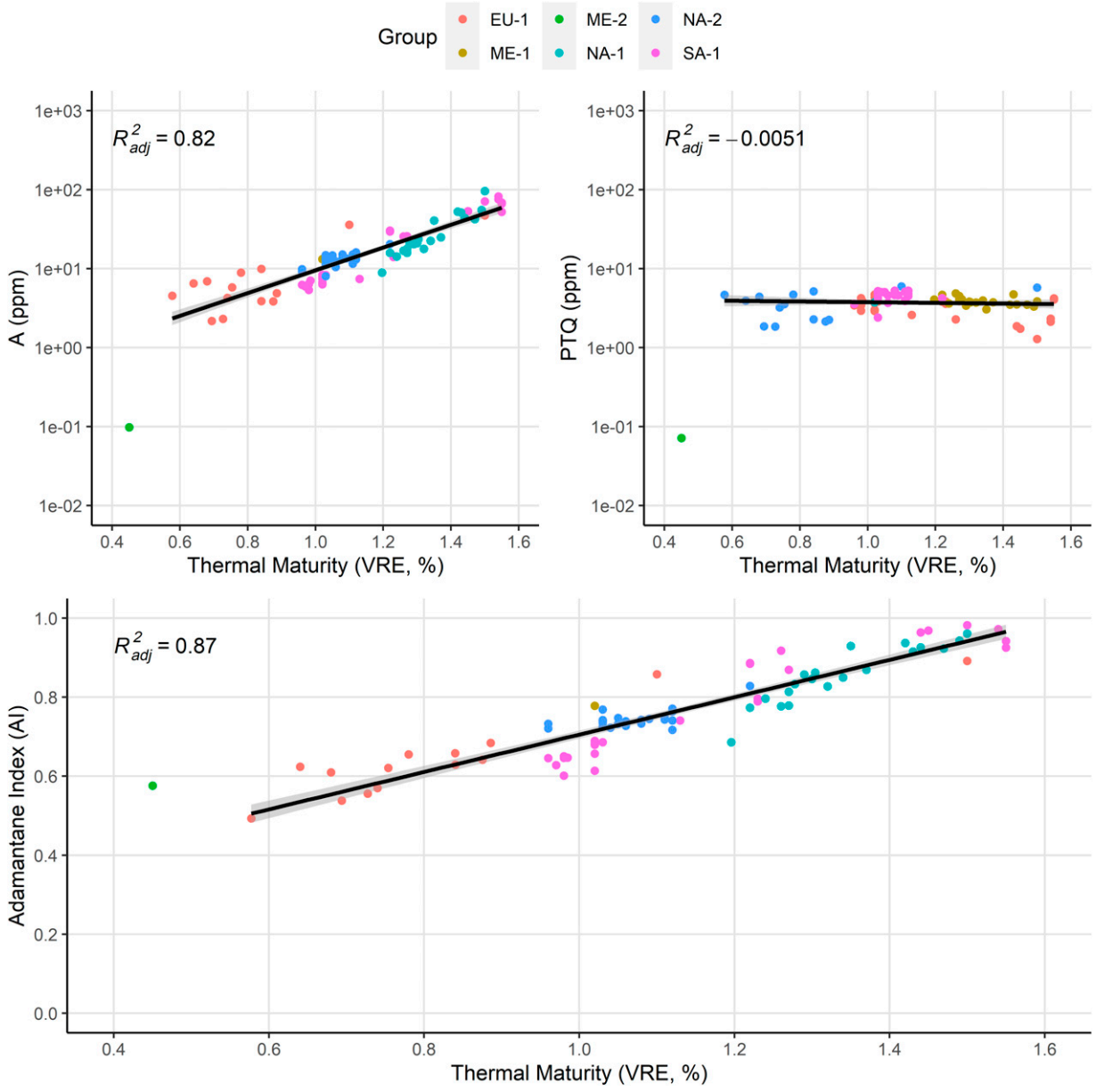

Figure 9. Concentrations of adamantane (A) and perhydrotriquinacene (PTQ) are shown together with the newly proposed adamantane index (AI) parameter versus thermal maturity for all fluids. Solid black lines represent linear fits to all data (excluding the outlier sample from the Middle East [ME]-2 group in green), with 95% confidence intervals of the fits in gray shading. EU = Europe; NA = North America; R^2_{adj} = adjusted coefficient of determination; SA = South America; VRE = vitrinite reflectance equivalent.

Crucially, our newly proposed AI parameter has a high linear correlation with thermal maturity across our full data set (adjusted coefficient of determination = 0.87), resulting in a better performance than the other diamondoid maturity indices that were previously established in the literature (Chen et al., 1996; Zhang et al., 2005; Mankiewicz et al., 2009). This enhanced sensitivity to maturity and its potentially global applicability make the AI parameter especially promising for predictive purposes. The corresponding equation for fluid maturity prediction using the AI parameter is

$$\text{AI-VRE}\ (\%) = 1.84 \times \text{AI} - 0.28 \quad (5)$$

Although the confidence interval of the linear regression model for the AI parameter is relatively tight, we recommend to apply an uncertainty of at least ±0.1% VRE to all fluid maturities predicted using this AI-VRE relationship.

DISCUSSION AND OUTLOOK

Based on our new calibration data set, the response of diamondoid concentrations to increasing thermal maturity is generally dependent on the size of the relevant compounds (Figure 2). Smaller diamondoids are consistently being generated across the oil window, whereas larger diamondoids are first generated and then destroyed beyond their optimal maturity regime. Previous studies using pyrolysis experiments had established similar patterns for adamantanes and diamantanes (Wei et al., 2006; Fang et al., 2012, 2013; Jiang et al., 2018), but to the best of our knowledge, this is the first time that this relationship is recorded in a series of naturally occurring fluids across the full adamantane to tetramantane spectrum. Our observations are in line with both theory and observations for other compound classes in petroleum fluids such as n-alkanes and biomarkers (Peters et al., 2005) but provide no further insights into the origins of diamondoids themselves. Hence, we recommend investigation of diamondoid formation pathways as a dedicated subject of future studies.

Our results show that most diamondoid indices work well as relative maturity indicators for fluids within a given basin, but not necessarily in all marine petroleum systems. Furthermore, our observation that adamantane-based indices perform better than diamantane-based indices over the studied fluid maturity range appears to be in accordance with previous work in which the methyldiamantane index parameter was shown to be a sensitive maturity parameter only beyond a VRE of ~2.0% (Fang et al., 2012). We expect that our newly proposed AI parameter will represent a major step forward in diamondoid-based quantitative maturity prediction across petroleum systems globally. A paired evaluation using the absolute abundances of adamantane and the various ethyladamantane isomers may prove especially useful. However, future validation of these parameters against other independent fluid data sets with good maturity control will be key. In addition, the applicability of the diamondoid maturity models presented here to fluids derived from type I and/or type III source rocks remains to be evaluated, albeit that access to sufficiently large and well-calibrated nonmarine data sets is very limited.

We acknowledge that many other maturity parameters are well-established with respect to petroleum systems analysis. Existing maturity parameters commonly work well, but typically only for a relatively small maturity window or a specific set of geological conditions. For example, sterane-based biomarker indices commonly reach parameter saturation at a VRE of ~0.8%, whereas most aromatic biomarker indices are only applicable at a VRE of ~1.0% and above (Peters et al., 2005). Thus, the main advantage of the diamondoid-based maturity models presented here is that they can be applied to crude oil and gas condensate fluids of all maturity levels. Moreover, our calibration data set is directly representative of naturally occurring petroleum fluids and not reliant on inferences from kerogen pyrolysis experiments.

To further develop the next generation of thermal maturity models for petroleum fluids, future studies could expand on our methods by including fluids from other source-rock types and depositional environments. Ideally, diamondoid data should be generated in conjunction with other established whole oil, saturate and aromatic biomarker, and gas fraction data types, so that these integrated data sets can be jointly inverted using statistical approaches for a potentially superior performance.

REFERENCES CITED

Atwah, I., J. M. Moldowan, D. Koskella, and J. Dahl, 2021, Application of higher diamondoids in hydrocarbon mudrock systems: Fuel, v. 284, 118994, 9 p., doi:10.1016/j.fuel.2020.118994.

Botterell, P. J., D. W. Houseknecht, P. G. Lillis, S. M. Barbanti, J. E. Dahl, and J. M. Moldowan, 2021, Geochemical advances in Arctic Alaska oil typing – North Slope oil correlation and charge history: Marine and Petroleum Geology, v. 127, 104878, 23 p., doi:10.1016/j.marpetgeo.2020.104878.

Chen, J., J. Fu, G. Sheng, D. Liu, and J. Zhang, 1996, Diamondoid hydrocarbon ratios: Novel maturity indices for highly mature crude oils: Organic Geochemistry, v. 25, no. 3–4, p. 179–190, doi:10.1016/S0146-6380(96)00125-8.

Cheng, X., D. Hou, and C. Xu, 2018, The effect of biodegradation on adamantanes in reservoired crude oils from the Bohai Bay Basin, China: Organic Geochemistry, v. 123, p. 38–43, doi:10.1016/j.orggeochem.2018.06.008.

Clark, T., T. M. Knox, M. A. McKervey, H. Mackle, and J. J. Rooney, 1979, Thermochemistry of bridged-ring substances. Enthalpies of formation of some diamondoid hydrocarbons and of perhydroquinacene: Comparisons with data from empirical force field calculations: Journal of the American Chemical Society, v. 101, no. 9, p. 2404–2410, doi:10.1021/ja00503a028.

Dahl, J. E., J. M. Moldowan, K. E. Peters, G. E. Claypool, M. A. Rooney, G. E. Michael, M. R. Mello, and M. L. Kohnen, 1999, Diamondoid hydrocarbons as indicators of natural oil cracking: Nature, v. 399, no. 6731, p. 54–57, doi:10.1038/19953.

Engler, E. M., M. Farcasiu, A. Sevin, J. M. Cense, and P. V. R. Schleyer, 1973, Mechanism of adamantane rearrangements: Journal of the American Chemical Society, v. 95, no. 17, p. 5769–5771, doi:10.1021/ja00798a059.

Esegbue, O., D. M. Jones, P. F. van Bergen, and S. Kolonic, 2020, Quantitative diamondoid analysis indicates oil cosourcing from a deep petroleum system onshore Niger Delta Basin: AAPG Bulletin, v. 104, no. 6, p. 1231–1259, doi:10.1306/0122201618217407.

Fang, C., Y. Xiong, Y. Li, Y. Chen, J. Liu, H. Zhang, T. A. Adedosu, and P. Peng, 2013, The origin and evolution of adamantanes and diamantanes in petroleum: Geochimica et Cosmochimica Acta, v. 120, p. 109–120, doi:10.1016/j.gca.2013.06.027.

Fang, C., Y. Xiong, Q. Liang, and Y. Li, 2012, Variation in abundance and distribution of diamondoids during oil cracking: Organic Geochemistry, v. 47, p. 1–8, doi:10.1016/j.orggeochem.2012.03.003.

Forkner, R., A. Fildani, J. Ochoa, and J. M. Moldowan, 2021, Linking source rock to expelled hydrocarbons using diamondoids: An integrated approach from the Northern Gulf of Mexico: Journal of Petroleum Science and Engineering, v. 196, 108015, 13 p., doi:10.1016/j.petrol.2020.108015.

Jiang, W., Y. Li, C. Fang, Z. Yu, and Y. Xiong, 2021, Diamondoids in petroleum: Their potential as source and maturity indicators: Organic Geochemistry, v. 160, 104298, 7 p., doi:10.1016/j.orggeochem.2021.104298.

Jiang, W., Y. Li, and Y. Xiong, 2018, The effect of organic matter type on formation and evolution of diamondoids: Marine and Petroleum Geology, v. 89, p. 714–720, doi:10.1016/j.marpetgeo.2017.11.003.

Landa, S., and V. Macháček, 1933, Sur l'adamantane, nouvel hydrocarbure extrait du naphte: Collection of Czechoslovak Chemical Contributions, v. 5, p. 1–5, doi:10.1135/cccc19330001.

Mankiewicz, P. J., R. J. Pottorf, M. G. Kozar, and P. Vrolijk, 2009, Gas geochemistry of the Mobile Bay Jurassic Norphlet Formation: Thermal controls and implications for reservoir connectivity: AAPG Bulletin, v. 93, no. 10, p. 1319–1346, doi:10.1306/05220908171.

Moldowan, J. M., J. Dahl, D. Zinniker, and S. M. Barbanti, 2015, Underutilized advanced geochemical technologies for oil and gas exploration and production-1. The diamondoids: Journal of Petroleum Science Engineering, v. 126, p. 87–96, doi:10.1016/j.petrol.2014.11.010.

Paquette, L. A., G. V. Meehan, and S. J. Marshall, 1969, Functionalization reactions of tricyclo[5.2.1.04,10]decane. The tricyclo[5.2.1.04,10]decane to adamantane rearrangement: Journal of the American Chemical Society, v. 91, no. 24, p. 6779–6784, doi:10.1021/ja01052a041.

Peters, K. E., C. C. Walters, and J. M. Moldowan, 2005, The biomarker guide: Cambridge, United Kingdom, Cambridge University Press, 1155 p.

R Core Team, 2022, R: A language and environment for statistical computing: Vienna, Austria, R Foundation for Statistical Computing, accessed August 1, 2022, https://www.R-project.org/.

Schneider, A., R. W. Warren, and E. J. Janoski, 1964, Formation of perhydrophenalenes and polyalkyladamantanes by isomerization of tricyclic perhydroaromatics: Journal of the American Chemical Society, v. 86, no. 23, p. 5365–5367, doi:10.1021/ja01077a087.

Schulz, L. K., A. Wilhelms, E. Rein, and A. S. Steen, 2001, Application of diamondoids to distinguish source rock facies: Organic Geochemistry, v. 32, no. 3, p. 365–375, doi:10.1016/S0146-6380(01)00003-1.

Spaak, G., D. S. Edwards, E. Grosjean, A. G. Scarlett, N. Rollet, and K. Grice, 2020, Identifying multiple sources of petroleum fluids in Browse Basin accumulations using diamondoids and semi-volatile aromatic compounds: Marine and Petroleum Geology, v. 113, 104091, 20 p., doi:10.1016/j.marpetgeo.2019.104091.

Wei, Z., J. M. Moldowan, D. M. Jarvie, and R. Hill, 2006, The fate of diamondoids in coals and sedimentary rocks: Geology, v. 34, no. 12, p. 1013–1016, doi:10.1130/G22840A.1.

Wei, Z., J. M. Moldowan, K. E. Peters, Y. Wang, and W. Xiang, 2007a, The abundance and distribution of diamondoids in biodegraded oils from the San Joaquin Valley: Implications for biodegradation of diamondoids in petroleum reservoirs: Organic Geochemistry, v. 38, no. 11, p. 1910–1926, doi:10.1016/j.orggeochem.2007.07.009.

Wei, Z., J. M. Moldowan, S. Zhang, R. Hill, D. M. Jarvie, H. Wang, F. Song, and F. Fago, 2007b, Diamondoid hydrocarbons as a molecular proxy for thermal maturity and oil cracking: Geochemical models from hydrous pyrolysis: Organic Geochemistry, v. 38, no. 2, p. 227–249, doi:10.1016/j.orggeochem.2006.09.011.

Whitlock, H. W., and M. W. Siefken, 1968, Tricyclo[4.4.0.03,8]decane to adamantane rearrangement: Journal of the American Chemical Society, v. 90, no. 18, p. 4929–4939, doi:10.1021/ja01020a028.

Wickham, H., 2009, ggplot2: Elegant graphics for data analysis: New York, Springer-Verlag, 213 p.

Williams, J. A., M. Bjorøy, D. L. Dolcater, and J. C. Winters, 1986, Biodegradation in South Texas Eocene oils—Effects on aromatics and biomarkers: Organic Geochemistry, v. 10, no. 1–3, p. 451–461, doi:10.1016/0146-6380(86)90045-8.

Zhang, S., H. Huang, Z. Xiao, and D. Liang, 2005, Geochemistry of Palaeozoic marine petroleum from the Tarim Basin, NW China. Part 2: Maturity assessment: Organic Geochemistry, v. 36, no. 8, p. 1215–1225, doi:10.1016/j.orggeochem.2005.01.014.